# The ESS linac

Eshraqi, Mohammad; Bustinduy, Ibon; Celona, Luigi; Comunian, Michele; Danared, Håkan; de Prisco, Renato; Grespan, Francesco; Lindroos, Mats; McGinnis, David; Miyamoto, Ryoichi; Møller, Søren Pape; Munoz, Mark; Ponton, Aurelian; Sargsyan, Edgar; Thomsen, Heine Dølrath

2014

# THE ESS LINAC

M. Eshraqi[1*], I. Bustinduy[2], L. Celona[3], M. Comunian[4], H. Danared[1], R. De Prisco[1,4], F. Grespan[4], M. Lindroos[1], D. McGinnis[1], R. Miyamoto[1], S. P. Møller[5], M. Munoz[1], A. Ponton[1], E. Sargsyan[1], H. D. Thomsen[5]. [1] ESS, Lund, Sweden, [2] ESS-Bilbao, Bilbao, Spain, [3] INFN-LNS, Catania, Italy, [4] INFN-LNL, Legnaro, Italy, [5] Arhus Univeristy, Arhus, Denmark

*Abstract*

The European Spallation Source, ESS, uses a linear accelerator to bombard the tungsten target with the high intensity protons beam for producing intense beams of neutrons. The nominal average beam power of the linac is 5 MW with a peak beam power at target of 125 MW. During last year the ESS linac cost was re-evaluated, and to meet the budget a few modifications were introduced to the linac design. One of the major changes is the reduction of the final energy from 2.5 GeV to 2.0 GeV and therefore beam current was increased accordingly to compensate for the lower final energy. As a result the linac is designed to meet the cost objective by taking a higher risk. This paper focuses on the driving forces behind the new design, engineering and beam dynamics requirements of the design and finally on the beam dynamics performance of the linac.

## INTRODUCTION

The high power linac of European Spallation Source, ESS, accelerates 62.5 mA of protons up to 2 GeV in a sequence of normal conducting and superconducting accelerating structures. These protons are to be used for the spallation process in which a high flux of pulsed neutrons will be generated in a neutron rich target material. The accelerator is a 5 MW proton linac delivering beams of energies up to 2.0 GeV to the target in long pulses of 2.86 ms with a repetition rate of 14 Hz − corresponding to a duty cycle of 4%. Pulse length and repetition rate are high level parameters and affect the design of the instruments and the neutron guides. Table 1 shows the differences of the 2013 baseline, code named OPTIMUSPLUS Fig. 1, and the 2012 baseline linac.

At a frequency of 352.21 MHz a 62.5 mA beam has $\sim 1.1 \times 10^9$ protons per bunch. From $\sim$ 200 MeV onward the acceleration is done at twice the frequency of the front end, 704.42 MHz, to improve the energy efficiency of the linac.

Hands-on maintenance and machine protection set limits, 1 W/m and 0.1 W/dm respectively, on beam losses and have been a concern in every high power linac. Therefore it is crucial, specially for high power accelerators, to design a linac which does not excite particles to beam halo.

Table 1: ESS Main Parameters

| Parameter | 2012 Baseline | 2013 Baseline |
|---|---|---|
| Ion species | Proton | Proton |
| Energy [GeV] | 2.5 | 2.0 |
| Beam power [MW] | 5 | 5 |
| Repetition rate [Hz] | 14 | 14 |
| Beam current [mA] | 50 | 62.5 |
| Beam pulse [ms] | 2.86 | 2.86 |
| Duty cycle [%] | 4 | 4 |

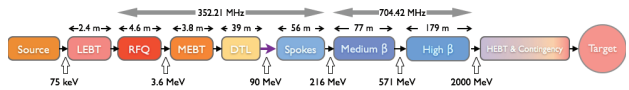


Figure 1: Block layout of the ESS baseline linac 2013, OptimusPlus (not to scale). Warm colored boxes represent the normal conducting components and cold color boxes the superconducting sections.

## ARCHITECTURE

### *Ion Source and LEBT*

The high intensity beam of protons is produced by a Microwave Discharge Ion Source, MDIS. The beam pulse generated by the proton source is up to 3 ms long with an energy of 75 keV and a proton intensity exceeding 80 mA at the source exit. These type of ion sources have a high reliability just shy of 100% and a long mean time between failures, MTBF. The high reliability of these sources has already been demonstrated in similar ion sources [1]. The source is followed by the low energy beam transport, LEBT, which is composed of two magnetic solenoids that match the beam to the downstream RFQ, a chopper system that removes low quality head and tail of the beam, an iris that is used to generate different (lower)beam currents, and a set of beam diagnostics that measures the beam before it is injected to the linac.

### *RFQ*

The four-vane RFQ as the first rf accelerating structure in the ESS linac, accelerates, focuses, and bunches the continuous 75 keV beam to 3.62 MeV within 4.6 m [2]. The output energy of the RFQ has increased in this layout from 3 MeV to 3.62 MeV in a process of optimizing all the transition energies in the linac. The beam current at the exit of the RFQ under nominal operation modes should be

* mamad.eshraqi@esss.se



ISBN 978-3-95450-132-8

62.5 mA, which taking into account the nominal transmission of 98%, the input beam should be at least 64 mA. The rf frequency of the RFQ and hence the bunches is 352.21 MHz. The peak electric fields on the vane surface has been limited to a Kilpatrick value of 1.8.

### *MEBT*

A medium energy beam transport between the RFQ and the DTL transports and matches the beam out of the former structure to the latter one, provides means to collimate the beam, measures the beam's transverse and longitudinal profile and chops off the remaining low quality bunches which couldn't have been cleaned out by the LEBT chopper. The MEBT is composed of 11 quadrupoles, three buncher cavities, a chopper with its correspondent dump system, 3 sets of 4 independent collimating plates and beam diagnostics.

### *DTL*

The drift tube linac brings the beam energy to 89.6 MeV in five tanks [3]. Each tank is fed by a 2.8 MW klystron, having left a 30% margin for LLRF, tuning and waveguide losses, 2.2 MW of power is delivered to the cavity via two rf windows, almost 50% of which is transferred to the beam. Higher input energy to the DTL resulted in longer input cells with several positive consequences; longer cells could house bigger quadrupoles reducing their magnetic gradient for the same integrated gradient, have longer gaps reducing the field at the flat of the drift tube due to magnets and also rf, and enhances the effective shunt impedance, ZTT. The transverse focusing is still provided by permanent magnet quadrupoles, PMQs, that are housed in every other drift tube. Three corrector dipoles per plane per tank are correcting the beam center. The constraints present in a DTL required an optimization process on where to put these corrector dipoles.

### *Spoke Section*

The DTL is the last normal conducting structure, and right after it comes the low energy differential pumping section, LEDP, that is used to create the required vacuum quality at the transition to superconducting cavities. The spoke cavities are used to accelerate the beam from 89.6 MeV to 216 MeV. One of the reasons for choosing spoke cavities instead of the conventional normalconducting structures in this energy range is their relatively large transverse aperture and tune-ability for different phase and energy beams. These 352.21 MHz double-spoke cavities with an optimum $\beta$ of 0.50 are housed in pairs in 13 cryomodules, and are separated by spoke warm units, SWU. Every SWU is composed of a pair of quadrupoles each being equipped with a single plane corrector and a beam position monitor, and a central slot allocated to beam diagnostics [5].

### *Elliptical Sections*

The rf frequency doubles to 704.42 MHz at the beginning of the next structure, the medium-$\beta$ elliptical cavities. There are two families of elliptical cavities accelerating the beam from the spoke output energy to 571 MeV using 36 medium-$\beta$ cavities and further to 2.0 GeV by 84 high-$\beta$ cavities. In both sections four cavities are housed in cryomodules of identical length. Having different geometric $\beta$s of 0.67 and 0.86 respectively, the medium-$\beta$ cavities are given an extra cell (6-cell) with respect to high-$\beta$ cavities (5-cell) to have almost the same length. This has been done to achieve the same period length in the medium and high-$\beta$ sections, making them swap-able in case the required gradient in medium-$\beta$ is not achieved. There are identical elliptical warm units, EWUs, before each cryomodule. These EWUs have the same functionality as SWUs, with bigger apertures, and longer quadrupoles. To have the same flexibility at the spoke to medium-$\beta$ transition the period lengths in elliptical section is chosen to be exactly twice that of the spoke section [5].

### *HEBT*

The same periodicity, in transverse plane, is maintained for 15 periods after the high-$\beta$ section in the high energy beam transport, HEBT, for contingency purposes. After this contingency area, there is one more EWU which is followed by a vertical dipole with a bending angle of 4° that also works as a switch magnet between the beam dump and the target. The beam going to the target is bent back to horizontal using a second vertical dipole after 6 periods of longer doublet focused sections that are adjusted to create an achromat dogleg. This beam is transported to the target using a set of quadrupoles and 8 raster magnets that paint the target surface in horizontal and vertical directions at different frequencies [4]. To reduce the beam center movement on target due to energy jitter the phase advance between the second dipole and the target surface is set to be a multiple 180°. A fixed collimator may intercept beam halo, protecting edges of the target, and also stops the back scattered neutrons from target. When the beam is directed to the 12.5 kW beam dump, the beam is magnified using three quadrupoles.

## BEAM DYNAMICS

### *Design Criteria*

In the latest design one of the main goals was to reduce the cost of the accelerator and that resulted in a linac with lower final energy, but higher current to keep the power constant. Increased beam current would have increased the effect of space-charge and therefore a study was performed to lower the effect of space-charge without increasing the cost [6]. Following this paper [6], the relative tune spread ($\zeta = 1 - \sigma/\sigma_0$), where $\sigma$ and $\sigma_0$ are the phase advances with and without current respectively, is kept below 0.6




ISBN 978-3-95450-132-8

(limiting the number of mismatch resonances to only two) while the current is increased by 25%, see Fig. 2.

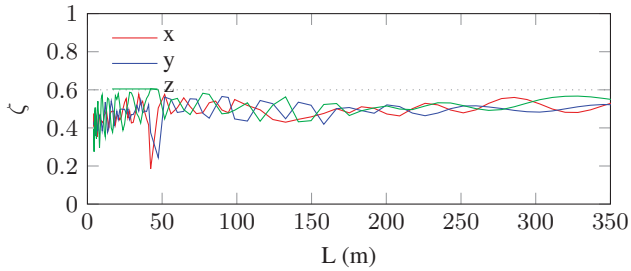


Figure 2: Relative tune spread along the linac, the dotted line marks the 0.6 limit.

The ESS linac will accelerate beam currents from 6.5 mA to 62.5 mA, therefore a smooth and monotonic variation of the phase advance per meter not only improves the matching, it also shortens the tuning time for different beam currents. On top of this, the structures are matched by smoothing the phase-advance variation at transitions to assure a good beam quality throughout the accelerator, even with different beam currents. The transverse phase advance per period is limited to 87° to reduce the percentage of the beam that due to their phase otherwise would have had a phase advance exceeding 90° per period. To improve the acceleration efficiency, the longitudinal phase advance per period is increased to 85° in the medium $\beta$ section, in the rest of the linac it has a lower value. On top of the transverse aperture, the longitudinal acceptance has also been kept large not to cause longitudinal losses which eventually result in transverse losses. The rf synchronous phase is plotted in Fig. 3.

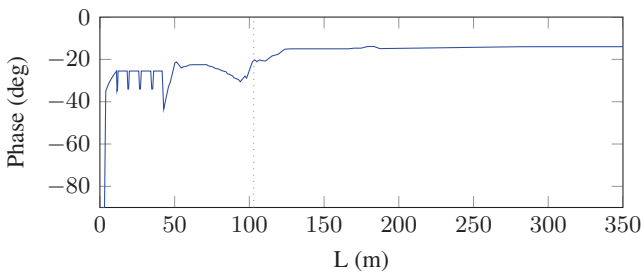


Figure 3: Synchronous phase along the linac, the dotted line marks the transition from spoke to medium $\beta$.

### *Simulations*

A gaussian beam in 4D, truncated at $4 \times \sigma$ is generated at the input of the RFQ with $100,000$ macro-particles. These beam has been tracked all the way through the linac to the target. The tracking is performed using the code TRACEWIN [7]. The PICNIC 3D space charge routine of the code is used to calculate the space-charge force of the beam using a $10 \times 10 \times 10$ mesh, and the kick is applied 15 times per $\beta \cdot \lambda$. Choosing a finer mesh or a higher number of space charge calculations does not affect the results noticeably and increases the CPU time. To model the superconducting cavities their one dimensional fieldmap on axis is used [5]. The RMS beam envelopes and emittance growth from the RFQ exit to the target is plotted are Fig. 4 and 5.

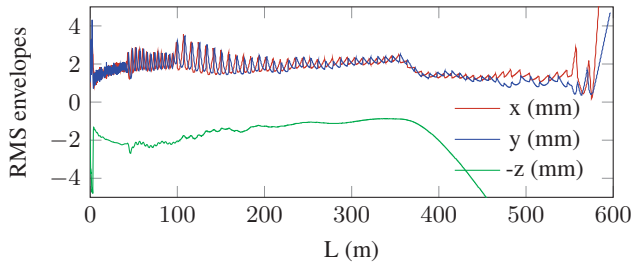


Figure 4: RMS envelopes from the RFQ exit to the target.

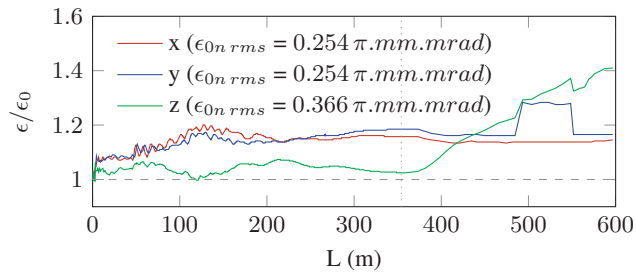


Figure 5: RMS emittance growth with respect to input beam along the linac and HEBT. Vertical dotted line shows the end of linac/start of HEBT.

## SUMMARY

The ESS linac has been redesigned to meet the budget constraints. The main changes were reduced energy and increased beam current to keep the power constant. Though an increase in beam current is associated with higher risk, beam dynamics design of the linac has been modified not to suffer from this higher current.

## REFERENCES

[1] L. Celona et al., Rev. Sci. Instrum. 75, 5 (2004).

[2] A. Ponton, "Note on the ESS RFQ Design Update", ESS Technical Report, 2014.

[3] R. D. Prisco, *et.al.*, "ESS DTL Status: Redesign and optimizations", *These proceedings*.

[4] H. D. Thomsen, *et al.*, IPAC'14, WEPRO073 (2014).

[5] M. Eshraqi, "Beam physics design of the Optimus+ SC linac", eval.esss.lu.se/DocDB/0003/000309/003/OptimusPlus.pdf.

[6] M. Eshraqi, J,-M, Lagniel, "On the choice of linac parameters for minimal beam losses", IPAC2013.

[7] R. Duperrier, N. Pichoff and D. Uriot, Proc. International Conf. on Computational Science, Amsterdam, The Netherlands, 2002.